Turkish Journal of Electrical Engineering & Computer Sciences

http://journals.tubitak.gov.tr/elektrik/

Research Article

Turk J Elec Eng & Comp Sci
(2019) 27: 675 – 684
© TÜBİTAK
doi:10.3906/elk-1803-97

Synchronization and antisynchronization protocol design of chaotic nonlinear gyros: an adaptive integral sliding mode approach

Fazal ur RAHMAN[1], **Qudrat KHAN**[2,*], **Rini AKMELIAWATI**[3]
[1]Department of Electrical Engineering, Capital University of Sciences, Islamabad, Pakistan
[2]Center for Advanced Studies in Telecommunications, COMSATS Institute of Information Technology, Islamabad, Pakistan
[3] Kulliyyah of Mechatronics Engineering, International Islamic University Malaysia, Kuala Lumpur, Malaysia

Received: 14.03.2018 • **Accepted/Published Online:** 29.11.2018 • **Final Version:** 22.01.2019

Abstract: A novel control protocol design, via integral sliding mode control with parameter update laws, for synchronization and desynchronization of a chaotic nonlinear gyro with unknown parameters is the focus of this work. The error dynamics of the actual system are substructured into nominal and uncertain parts to employ adaptive integral sliding mode (AISM) control. The uncertain parameters are estimated via devised adaptive laws. Then the disagreement dynamics are guided to origin via AISM control. The stabilizing controller is also designed in terms of nominal control along with a compensating component. The control and the parameter update laws are constructed to ensure the strictly negative derivative of a Lyapunov function. Graphical results related to synchronization, desynchronization, and chaos suppression are displayed to demonstrate the potential of the proposed control.

Key words: Chaotic gyro, synchronization, desynchronization, adaptive backstepping method, AISM control, Lyapunov function

1. Introduction

One of the fascinating areas among researchers is the study of chaotic systems. It has been focused on since the innovative chaos control of Ott et al. [1] and synchronization protocol of Pecora and Carroll [2]. In this context, the methodologies devised in [3–5] attracted a wide number of researchers and, consequently, this area became an active topic in nonlinear science. In [6] only a partial state of the chaotic system, accompanied by the inherent dynamic properties of the chaotic systems, was utilized to synchronize coupled systems. An adaptive backstepping approach accompanied by a tuning function was proposed in [7] to synchronize uncertain continuous time chaotic systems and to confirm global asymptotic synchronization. A recursive adaptive backstepping technique was proposed in [8] and the control law was constructed, which supported the chaotic system to synchronize asymptotically. The active control technique in [9] regulated the synchronization error of two dissimilar chaotic systems. A very similar problem was solved in [10] by applying stability theory and the gain area of the controller was determined. A finite time stability theory-based controller was designed in [11] and the synchronization of two dissimilar chaotic systems was reached. The finite time stability results in precision; however, the robustness degrades in this strategy. An advanced backstepping oriented control was proposed to achieve synchrony of uncertain chaotic systems [12] and antisynchronization was reached in [13]. A

*Correspondence: qudratullah@gmail.com

neural network (NN)-based strategy was proposed in [14], where the NNs are synthesized with dynamic surface control. This control strategy confirms the robust asymptotic synchronization. It is worth mentioning that in real applications chaotic systems work under external disturbances and unmodeled dynamics. In such cases, the influence of the aforementioned strategies is degraded.

In order to deal with chaotic systems' synchronization/antisynchronization more suitably, some researchers have focused on sliding mode control (SMC)-based solutions to the aforesaid problems (see, for instance, [15–18]). SMC remains sensitive to disturbances in reaching phase and it also suffers from the famous chattering phenomenon in sliding. In order to get rid of these issues a number of researchers have focused on reaching phase-free SMC with alleviated vibrations and provoked robustness [19–22]. In this work, the authors have focused on robustness enhancement against the parametric uncertainties of a nonlinear gyro system. The contribution of this work is twofold: first, the development of the adaptive law for the parameter estimations, which confirms the asymptotic convergence of the parameters to their actual values, and second, the development of an integral sliding mode strategy for the referred chaotic nonlinear system. Closed-loop stability in the presence of parametric variations and matched disturbances is verified in the form of two theorems, which are further verified via simulation results. The problem of chaos suppression, synchronization, and antisynchronization are handled in this work via the proposed control law. In addition, the simulation results for chaos suppression and synchronization are compared with the standard literature [23] to highlight the benefits of our proposed strategy. In Section 2, the system description of the gyro system is presented. In Section 3, chaos suppression is considered under the action of the proposed adaptive control law. In Section 4, the synchronization and desynchronization of a master and slave system subjected to the newly proposed strategy is discussed. The system under study is simulated with the designed control laws and the results are presented in Section 5. In Section 6, conclusive remarks are presented.

2. System description of a nonlinear gyro

The nonlinear gyroscope model, which is employed in aerospace engineering [24], generally exhibits chaotic behavior. Its usage is also observed heavily in smart brakes systems of current automotive vehicles. The equation governing the dynamics of the nonlinear gyro, enriched with linear and nonlinear smoothening terms [24], is given by

$$\dot{x}_1 = x_2,$$

$$\dot{x}_2 = -\frac{\alpha(1-\cos x_1)^2}{\sin^3 x_1} - ax_2 - bx_2^3 + \beta\sin x_1 + f\sin(\omega t)\sin(x_1), \tag{1}$$

where x_1 represents the angular position and x_2 represents the angular velocity of the given system, and α, β, a, b, and f are the unknown parameters. Note that the dynamic system of Eq. ((1)) demonstrates chaotic behavior when $\alpha = 100$, $\beta = 1$, $a = 0.5$, $b = 0.05$, $\omega = 2$, and $f = 35.5$. Therefore, while assuming this system with different initial conditions, i.e. $(x_1, x_2) = (1, -1)$ and $(x_1, x_2) = (1, -1.02)$, the phase portraits are displayed in Figures 1 and 2. These figures show that the chaotic system's behavior varies as the set of initial conditions varies. The control and parameter update expressions are designed in detail in the subsequent section.

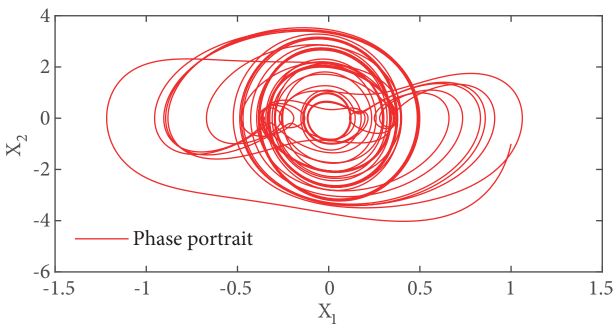

Figure 1. The phase portrait of the system with initial conditions $(x_1, x_2) = (1, -1)$.

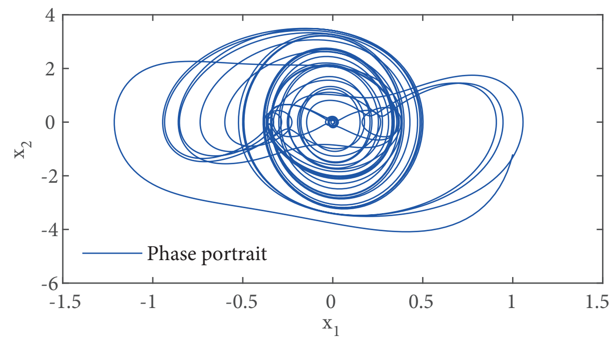

Figure 2. The phase portrait of the system with initial conditions $(x_1, x_2) = (1, -1.2)$.

3. Controlling chaos in gyroscope system

An adaptive integral sliding mode for suppressing chaos in the given gyroscopic mode is worked out in this section. A control signal $u(t)$ is introduced in Eq. ((1)) subject to the following assumption.

Assumption 1 *Assume that the parameters are unknown.*

Let $\hat{a}$, $\hat{b}$, $\hat{f}$, $\hat{\beta}$, $\hat{\alpha}$ be estimates of the parameters a, b, f, β, α, and $\tilde{a} = \alpha - \hat{a}$, $\tilde{b} = b - \hat{b}$, $\tilde{f} = f - \hat{f}$, $\tilde{\beta} = \beta - \hat{\beta}$, $\tilde{\alpha} = \alpha - \hat{\alpha}$ be the errors in estimations of a, b, f, β, α, respectively. Now the system of Eq. ((1)) in the presence of a control input u can be written as:

$$\dot{x}_1 = x_2,$$

$$\dot{x}_2 = -\frac{(\hat{\alpha}+\tilde{\alpha})(1-\cos x_1)^3}{\sin^3 x_1} - (\hat{a}+\tilde{a})x_2 - (\hat{b}+\tilde{b})x_2^3 + (\hat{\beta}+\tilde{\beta})\sin x_1 + (\hat{f}+\tilde{f})\sin(\omega t)\sin(x_1) + u + \delta, \tag{2}$$

where δ is matched uncertainty that enters through the input channel. Now the main task is to choose the input u. Therefore, choosing

$$u = \frac{\hat{\alpha}(1-\cos x_1)^2}{\sin^3 x_1} + \hat{a}x_2 + \hat{b}x_2^3 - \hat{\beta}\sin x_1 - \hat{f}\sin(\omega t)\sin(x_1) + v, \tag{3}$$

the system of Eq. ((2)) under the influence of input v takes the following form:

$$\dot{x}_1 = x_2,$$

$$\dot{x}_2 = -\frac{\tilde{\alpha}(1-\cos x_1)^2}{\sin^3 x_1} - \tilde{a}x_2 - \tilde{b}x_2^3 + \tilde{\beta}\sin x_1 + \tilde{f}\sin(\omega t)\sin(x_1) + v + \delta. \tag{4}$$

To employ integral sliding mode, choose the nominal system for Eq. ((3)) as:

$$\dot{x}_1 = x_2,$$

$$\dot{x}_2 = v_0, \tag{5}$$

where v_0 is the control input, which drives the nominal system. The first objective is to stabilize the nominal system of Eq. ((5)). Therefore, by defining a sliding surface $\sigma_0 = x_1 + x_2$ and calculating its time derivative along Eq. ((5)), one may have $\dot{\sigma_0} = \dot{x_1} + \dot{x_2} = x_2 + v_0$. Now, by choosing $v_0 = -x_2 - k\sigma_0, k > 0$, one may obtain $\dot{\sigma_0} = -k\sigma_0$, which proves asymptotic regulation of Eq. ((5)). Having stabilized Eq. ((5)), we proceed to the stabilization of Eq. ((4)) by defining an integral manifold of the following form:

$$\sigma = \sigma_0 + z = x_1 + x_2 + z. \tag{6}$$

The time derivative of Eq. ((6)) along Eq. ((4)) yields

$$\dot{\sigma} = \dot{x_1} + \dot{x_2} + \dot{z}$$

$$= x_2 - \frac{\tilde{\alpha}(1-\cos x_1)^2}{\sin^3 x_1} - \tilde{a}x_2 - \tilde{b}x_2^3 + \tilde{\beta}\sin x_1 + \tilde{f}\sin(\omega t)\sin(x_1) + v_0 + v_s + \delta + \dot{z}. \tag{7}$$

Note that z represents an integral term whose computation will be elaborated latter. Furthermore, the initial condition $z(0)$ will be chosen such that one may obtain $\sigma(0) = 0$. The control input is subdivided into two parts, i.e. $v = v_0 + v_s$, where v_0 and v_s are the nominal and compensating inputs, respectively. Their design will be outlined later. Now the problem we want to solve is the design of an adaptive protocol that ensures the asymptotic convergence of Eq. ((4)). This can be confirmed by stating the following theorem while choosing a Lyapunov function $v = \frac{1}{2}(\sigma^2 + \tilde{a^2} + \tilde{b^2} + \tilde{f^2} + \tilde{\alpha^2} + \tilde{\beta^2})$, with the adaptive laws for $\tilde{a}$, $\hat{a}$, $\tilde{b}$, $\hat{b}$, $\tilde{f}$, $\hat{f}$, $\tilde{\beta}$, $\hat{\beta}$, $\tilde{\alpha}$, $\hat{\alpha}$ and a mathematical expression for v_s which may result in $\dot{v} < 0$.

Theorem 1 *The states of the system of Eq. ((4)) approach the origin asymptotically if the adaptive laws for $\tilde{a}$, $\hat{a}$, $\tilde{b}$, $\hat{b}$, $\tilde{f}$, $\hat{f}$, $\tilde{\beta}$, $\hat{\beta}$, $\tilde{\alpha}$, $\hat{\alpha}$ and the value of v_s are chosen as follows:*

$$\dot{z} = -x_2 - v_0, v_s = -K1(\sigma + W sign(\sigma))$$

$$\dot{\tilde{a}} = \sigma x_2 - k_1\tilde{a}, \dot{\hat{a}} = -\dot{\tilde{a}}$$

$$\dot{\tilde{b}} = \sigma x_2^3 - k_2\tilde{b}, \dot{\hat{b}} = -\dot{\tilde{b}}$$

$$\dot{\tilde{f}} = -\sigma\sin(\omega t)\sin x_1 - k_3\tilde{f}, \dot{\hat{f}} = -\dot{\tilde{f}}$$

$$\dot{\tilde{\beta}} = -\sigma\sin x_1 - k_4\tilde{\beta}, \dot{\hat{\beta}} = -\dot{\tilde{\beta}}$$

$$\dot{\tilde{\alpha}} = \sigma\frac{(1-\cos x_1)^2}{\sin^3 x_1} - k_5\tilde{\alpha}, \dot{\hat{\alpha}} = -\dot{\tilde{\alpha}}, k, k_i > 0, i = 1, 2, ...5 \tag{8}$$

Proof To prove the aforesaid claim, consider a Lyapunov function $v = \frac{1}{2}(\sigma^2 + \tilde{a^2} + \tilde{b^2} + \tilde{f^2} + \tilde{\alpha^2} + \tilde{\beta^2})$. Calculating the time derivative of this function along Eq. ((7)), one may have

$$\dot{v} = \sigma\dot{\sigma} + \tilde{a}\dot{\tilde{a}}, \tilde{b}\dot{\tilde{b}} + \tilde{f}\dot{\tilde{f}} + \tilde{\alpha}\dot{\tilde{\alpha}} + \tilde{\beta}\dot{\tilde{\beta}}$$

$$= \sigma\{x_2 - \frac{\tilde{\alpha}(1-\cos x_1)^2}{\sin^3 x_1} - \tilde{a}x_2 - \tilde{b}x_2^3 + \tilde{\beta}\sin x_1 + \tilde{f}\sin(\omega t)\sin x_1 + v_0 + v_s + \delta + \dot{z}\} + \tilde{a}\dot{\tilde{a}} + \tilde{b}\dot{\tilde{b}} + \tilde{f}\dot{\tilde{f}} + \tilde{\alpha}\dot{\tilde{\alpha}} + \tilde{\beta}\dot{\tilde{\beta}}$$

$$= \sigma\Big(x_2+v_0+v_s+\delta+\dot{z}\Big)+\tilde{a}\{\dot{\tilde{a}}-\sigma x_2\}+\tilde{b}\{\dot{\tilde{b}}-\sigma x_2^3\}+\tilde{f}\{\dot{\tilde{f}}+\sigma\sin(\omega t)\sin x_1\}+\tilde{\alpha}\{\dot{\tilde{\alpha}}-\sigma\frac{(1-\cos x_1)^2}{\sin^3 x_1}\}+\tilde{\beta}\{\dot{\tilde{\beta}}+\sigma\sin x_1\}. \tag{9}$$

By using Eq. ((8)) in Eq. ((9)), we get the following:

$$\dot{v} = -K1(\sigma^2 + W|\sigma|) - k_1\tilde{a}^2 - k_2\tilde{b}^2 - k_3\tilde{f}^2 - k_4\tilde{\beta}^2 - k_5\tilde{\alpha}^2, \tag{10}$$

where $K_1 > |\delta|$ and $0 < W < 1$. Note that Eq. ((10)) guarantees that the variables and errors of the parameters converge to zero, or precisely σ, $\tilde{a}$, $\tilde{b}$, $\tilde{f}$, $\tilde{\beta}$, $\tilde{\alpha} \to 0$. This confirms the overlap of estimated parameters with true values. In addition, when $\sigma \to 0$, it ensures the establishment of integral sliding modes. In integral sliding modes, the system is under the action of the nominal control law v_0 and the uncertainties are compensated via the parameters of the update laws and the control component v_s. As already mentioned, in sliding mode, the nominal system works under the influence of v_0, can confirms that Eq. ((4)) approaches the origin, i.e. $x_1 \to 0$ and $x_2 \to 0$. In the next section, the aforesaid strategy is employed for the synchronization and desynchronization of two monovular systems. □

4. Synchronization (desynchronization) in the case of unknown parameters

The synchronization and desynchronization of two monovular nonlinear gyroscopes with uncertain parameters is achieved by employing an AISM control method. Take the master system with the governing dynamics of the form

$$\dot{x_1} = x_2,$$

$$\dot{x_2} = -\frac{(\hat{\alpha}+\tilde{\alpha})(1-\cos x_1)^2}{\sin^3 x_1} - (\hat{a}+\tilde{a})x_2 - (\hat{b}+\tilde{b})x_2^3 + (\hat{\beta}+\tilde{\beta})\sin x_1 + (\hat{f}+\tilde{f})\sin(\omega t)\sin(x_1), \tag{11}$$

and the slave system's dynamics as follows:

$$\dot{y_1} = y_2,$$

$$\dot{y_2} = -\frac{(\hat{\alpha}+\tilde{\alpha})(1-\cos y_1)^2}{\sin^3 y_1} - (\hat{a}+\tilde{a})y_2 - (\hat{b}+\tilde{b})y_2^3 + (\hat{\beta}+\tilde{\beta})\sin y_1 + (\hat{f}+\tilde{f})\sin(\omega t)\sin(y_1) + u + \delta. \tag{12}$$

The disagreement variables between Eqs. ((11)) and ((12)) are clearly characterized as:

$$e_1 = y_1 - qx_1,$$

$$e_2 = y_2 - qx_2. \tag{13}$$

Note that in Eq. ((13)), when one chooses $q = 1$, it results in synchronization, whereas the choice $q = -1$ comes up with antisynchronization. Based on the error variable defined in Eq. ((13)), the error dynamics can be calculated as follows:

$$\dot{e_1} = \dot{y_1} - q\dot{x_1} = y_2 - qx_2 = e_2,$$

$$\dot{e_2} = \dot{y_2} - q\dot{x_2}$$

$$= -\frac{(\hat{\alpha}+\tilde{\alpha})(1-\cos y_1)^2}{\sin^3 y_1} - (\hat{a}+\tilde{a})y_2 - (\hat{b}+\tilde{b})y_2^3 + (\hat{\beta}+\tilde{\beta})\sin y_1 + (\hat{f}+\tilde{f})\sin(\omega t)\sin(y_1) + u + \delta$$

$$-q\{-\frac{(\hat{\alpha}+\tilde{\alpha})(1-\cos x_1)^2}{\sin^3 x_1} - (\hat{a}+\tilde{a})x_2 - (\hat{b}+\tilde{b})x_2^3 + (\hat{\beta}+\tilde{\beta})\sin x_1 + (\hat{f}+\tilde{f})\sin(\omega t)\sin(x_1)\}. \quad (14)$$

Now, following the same procedure as outlined in Section 3, one can choose the control laws as follows:

$$u = \frac{\hat{\alpha}(1-\cos y_1)^2}{\sin^3 y_1} + \hat{a}y_2 + \hat{b}y_2^3 - \hat{\beta}\sin y_1 - \hat{f}\sin(\omega t)\sin(y_1) + q\{-\frac{\hat{\alpha}(1-\cos x_1)^2}{\sin^3 x_1} - \hat{a}x_2 - \hat{b}x_2^3$$

$$+\hat{\beta}\sin x_1 + \hat{f}\sin(\omega t)\sin(x_1)\} + v. \quad (15)$$

Now the new control input v is responsible for governing the following dynamic system:

$$\begin{aligned}\dot{e_1} =& e_2,\\ \dot{e_2} =& v + \delta - \frac{\tilde{\alpha}(1-\cos y_1)^2}{\sin^3 y_1} - \tilde{a}y_2 - \tilde{b}y_2^3 + \tilde{\beta}\sin y_1 + \tilde{f}\sin(\omega t)\sin(y_1) - q\{-\frac{\tilde{\alpha}(1-\cos x_1)^2}{\sin^3 x_1} - \tilde{a}x_2\\ &- \tilde{b}x_2^3 + \tilde{\beta}\sin x_1 + \tilde{f}\sin(\omega t)\sin(x_1)\}\end{aligned}$$

or

$$\begin{aligned}\dot{e_1} =& e_2,\\ \dot{e_2} =& v + \delta - \tilde{\alpha}\{\frac{(1-\cos y_1)^2}{\sin^3 y_1} - q\frac{(1-\cos x_1)^2}{\sin^3 x_1}\} - \tilde{a}\{y_2 - qx_2\} - \tilde{b}\{y_2^3 - qx_2^3\} + \tilde{\beta}\{\sin y_1 - q\sin x_1\}\\ &+ \tilde{f}\{\sin(\omega t)\sin y_1 - q\sin(\omega t)\sin x_1\}. \quad (16)\end{aligned}$$

The nominal system corresponding to the system of Eq. ((16)) is given by

$$\begin{aligned}\dot{e_1} &= e_2,\\ \dot{e_2} &= v_0. \quad (17)\end{aligned}$$

Now, by defining a new variable $\sigma_0 = e_1 + e_2$ and calculating its time derivation along Eq. ((17)), one may have $\dot{\sigma_0} = \dot{e_1} + \dot{e_2} = e_2 + v_0$. By selecting $v_0 = -e_2 - k\sigma, k > 0$, one may have $\dot{\sigma_0} = -k\sigma_0$, which guarantees the asymptotic convergence of Eq. ((17)). Now, to move ahead to the controlled input design, an integral manifold is furnished as follows:

$$\sigma = \sigma_0 + z = e_1 + e_2 + z, \quad (18)$$

where z is an integral term that helps in the reaching phase elimination. To observe sliding mode at time $t = 0$, the initial condition of the integral term dynamics, i.e. $z(0)$, will be chosen in such a way that it results in $\sigma(0) = 0$. The time derivative of Eq. ((18)) along Eq. ((16)), while substituting $v = v_0 + v_s$, looks as follows:

$$\begin{aligned}\dot{\sigma} =& \dot{e_1} + \dot{e_2} + \dot{z}\\ =& e_2 - \tilde{\alpha}\{\frac{(1-\cos y_1)^2}{\sin^3 y_1} - q\frac{(1-\cos x_1)^2}{\sin^3 x_1}\} - \tilde{a}\{y_2 - qx_2\} - \tilde{b}\{y_2^3 - qx_2^3\} + \tilde{\beta}\{\sin y_1 - q\sin x_1\}\\ &+ \tilde{f}\{\sin(\omega t)\sin y_1 - q\sin(\omega t)\sin x_1\} + v_0 + v_s + \dot{z}.\end{aligned}$$

At this stage, the main objective is the enforcement of the sliding mode along with the estimation of the uncertain parameters. This can be confirmed by stating Theorem 2.

Theorem 2 *The states of the system of Eq. ((16)) approach the origin asymptotically if the adaptive laws for* $\tilde{a}$, $\hat{a}$, $\tilde{b}$, $\hat{b}$, $\tilde{f}$, $\hat{f}$, $\tilde{\beta}$, $\hat{\beta}$, $\tilde{\alpha}$, $\hat{\alpha}$ *and the value of* v_s *are chosen as follows:*

$$\dot{z} = -e_2 - v_0, \quad v_s = -K_1(\sigma + W sign(\sigma))\dot{\tilde{a}} = \sigma(y_2 - qx_1) - k_1\tilde{a}, \quad \dot{\hat{a}} = -\dot{\tilde{a}}$$

$$\dot{\tilde{b}} = \sigma(y_2^3 - qx_2^3) - k_2\tilde{b}, \quad \dot{\hat{b}} = -\dot{\tilde{b}}$$

$$\dot{\tilde{f}} = -\sigma(\sin(\omega t)\sin y_1 - q\sin(\omega t)\sin x_1) - k_3\tilde{f}, \quad \dot{\hat{f}} = -\dot{\tilde{f}}$$

$$\dot{\tilde{\beta}} = -\sigma(\sin y_1 - q\sin x_1) - k_4\tilde{\beta}, \quad \dot{\hat{\beta}} = -\dot{\tilde{\beta}}$$

$$\dot{\tilde{\alpha}} = \sigma[\frac{(1-\cos y_1)^2}{\sin^3 y_1} - q\frac{(1-\cos x_1)^2}{\sin^3 x_1}] - k_5\tilde{\alpha}, \dot{\hat{\alpha}} = -\dot{\tilde{\alpha}}, k, k_i > 0, i = 1, 2, ...5. \tag{19}$$

Proof To prove the aforesaid claim, consider a Lyapunov function $v = \frac{1}{2}(\sigma^2 + \tilde{a^2} + \tilde{b^2} + \tilde{f^2} + \tilde{\alpha^2} + \tilde{\beta^2})$. Calculating the time derivative of this function along Eq. ((19)), one may have

$$\begin{aligned}
\dot{v} =& \sigma\dot{\sigma} + \tilde{a}\dot{\tilde{a}} + \tilde{b}\dot{\tilde{b}} + \tilde{f}\dot{\tilde{f}} \\
&+ \tilde{\beta}\dot{\tilde{\beta}} + \tilde{\alpha}\dot{\tilde{\alpha}} \\
&\sigma\{e_2 - \tilde{\alpha}\frac{(1-\cos y_1)^2}{\sin^3 y_1} - q\frac{(1-\cos x_1)^2}{\sin^3 x_1}\} - \tilde{a}\{y_2 - qx_2\} - \tilde{b}\{y_2^3 - qx_2^3\} + \tilde{\beta}\{\sin y_1 - q\sin x_1\} \\
&+ \tilde{f}\{\sin(\omega t)\sin y_1 - q\sin(\omega t)\sin x_1\} + v_0 + v_s + \delta + \dot{z} + \tilde{a}\dot{\tilde{a}} + \tilde{b}\dot{\tilde{b}} \\
&+ \tilde{f}\dot{\tilde{f}} + \tilde{\alpha}\dot{\tilde{\alpha}} + \tilde{\beta}\dot{\tilde{\beta}} \\
=& \sigma\{e_2 + v_0 + v_s + \delta\dot{z}\} + \tilde{a}\{\dot{\tilde{a}} - \sigma(y_2 - qx_2)\} + \tilde{b}\{\dot{\tilde{b}} - \sigma(y_2^3 - qx_2^3)\} + \tilde{f}\{\dot{\tilde{f}} + \sigma(\sin(\omega t)\sin y_1 - q\sin(\omega t)\sin x_1)\}
\end{aligned} \tag{20}$$

$$+\tilde{\beta}\{\dot{\tilde{\beta}} + \sigma(\sin y_1 - q\sin x_1)\} + \tilde{\alpha}\{\dot{\tilde{\alpha}} - \sigma[\frac{(1-\cos y_1)^2}{\sin^3 y_1}\} - q\frac{(1-\cos x_1)^2}{\sin^3 x_1}.]\} \tag{21}$$

Using Eq. ((19)) in Eq. ((21)) leads to

$$\dot{v} = -K1(\sigma^2 + W|\sigma|) - k_1\tilde{a}^2 - k_2\tilde{b}^2 - k_3\tilde{f}^2 - k_4\tilde{\beta}^2 - k_5\tilde{\alpha}^2. \tag{22}$$

This expression, like the statement in Theorem 1, guarantees that the error variables and errors of the parameters converge to zero, i.e. σ, $\tilde{a}$, $\tilde{b}$, $\tilde{f}$, $\tilde{\beta}$, $\tilde{\alpha} \to 0$. This confirms the true estimation of the parameters of the plant, and when $\sigma \to 0$, it ensures the establishment of integral sliding modes. In integral sliding modes, the system is under the action of the nominal control law v_0 and the uncertainties are compensated via the parameter update laws and the control component v_s. Under the action of v_0 error variables the system of Eq. ((16)) approaches the origin, i.e. $e_1 \to 0$ and $e_2 \to 0$. Consequently, the synchronization and antisynchronization of the two monovular systems occurs. The next section outlines the simulation results related to chaos suppression, synchronization, and desynchronization. □

5. Numerical simulations

The chaos suppression, synchronization, and antisynchronization results are discussed here. In the case of chaos suppression, the system is initialized with $(x_1(0), x_2(0)) = (1, -1)$. The states and parameter convergence of the system of Eq. ((4)) under the influence of the control laws of Eqs. ((3)), v_0, and ((8)) are shown in Figures 3–5. In Figure 3 the results of the proposed technique are compared with the standard literature results [23]. It is evident that the response of adaptive ISMC is oscillation-free, whereas the chaos suppression via the backstepping strategy [23] suffers from substantial oscillation. It is worth mentioning that adaptive ISMC was employed for the chaotic system, which was operated with matched uncertainty, i.e. $0.5\sin(t)$. This shows the robust and oscillation-free behavior of adaptive ISMC. During the synchronization of the two systems, the master system is excited from $(x_1(0), x_2(0)) = (1, -1)$ and the slave system is activated from $(y_1(0), y_2(0)) = (1, -1.2)$ under the action of the aforementioned matched uncertainty. The disagreement dynamics of Eq. ((16)) are simulated under the action of Eqs. ((15)), v_0 and ((19)). By choosing the scaling parameter $q = 1$, the synchronization occurs and the disagreement becomes zero. The corresponding results are pictured in Figures 6 and 7. In addition, the synchronization errors are compared in Figure 8 with results of [23]. The developed results under the proposed adaptive ISMC show quite fast convergence even when being initialized from the bigger values as compared to its counterpart [23]. This confirms the robust performance of the proposed technique. The desynchronization results are achieved by choosing the scaling parameter $q = -1$. The corresponding results are demonstrated in Figures 9 and 10. Note that the true values of the parameters in all simulation cases were set to be $a = 0.5$, $b = 0.05$, $f = 35.5$, $\beta = 1$, $\alpha = 100$, and $\omega = 2$.

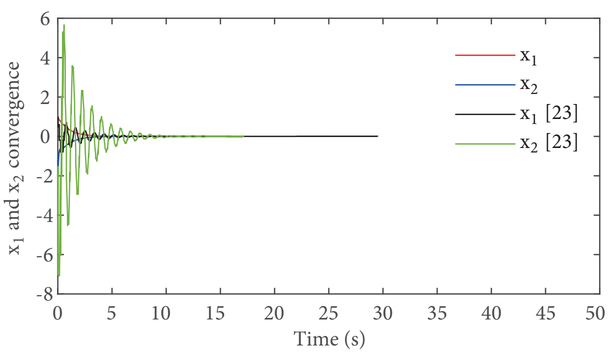

Figure 3. The chaos suppression via adaptive ISMC and backstepping law [23] when the system is initialized from $(x_1, x_2) = (1, -1.5)$.

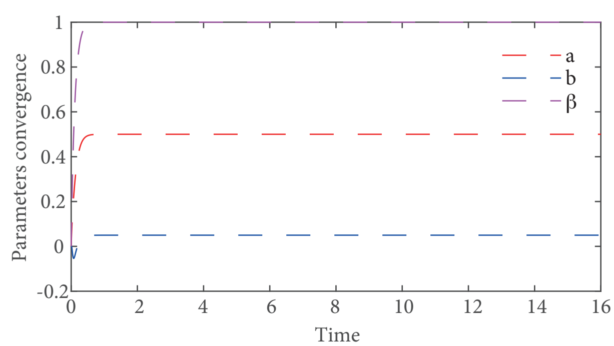

Figure 4. The approach of estimated a, b, β to the true values.

6. Conclusions

The chaos alleviation, synchronization, and desynchronization of two monovular chaotic gyros with uncertain plant parameters were attained by utilizing an AISM control. The unknown parameters are estimated by defining proper parameter update laws. To avoid the chattering phenomenon, a smooth continuous compensator is designed instead of the traditional discontinuous control. The compensator-based controller and adaptation laws were equipped to ensure Lyapunov function-based stability. The strength of this new control scheme was validated by MATLAB-generated results.

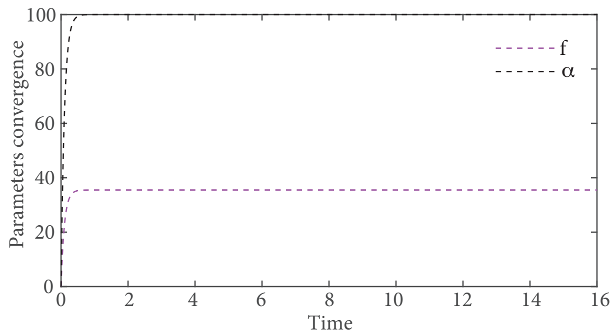

Figure 5. The approach of estimated f, α to the true values.

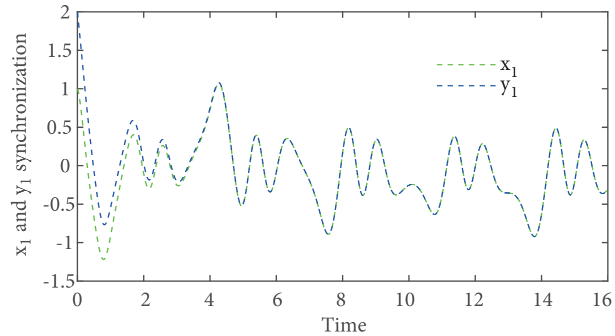

Figure 6. The synchronization of the state variables of the two monovular systems via adaptive ISMC.

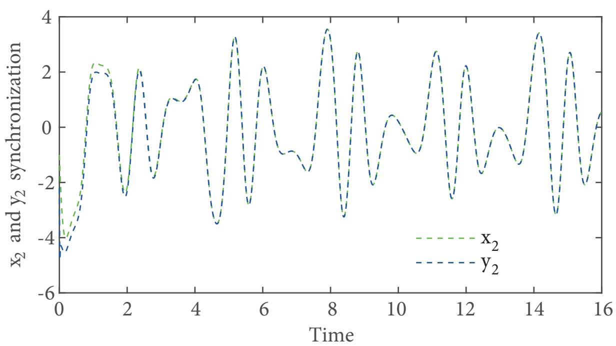

Figure 7. The synchronization of the velocities of the two monovular systems under the action of adaptive ISMC.

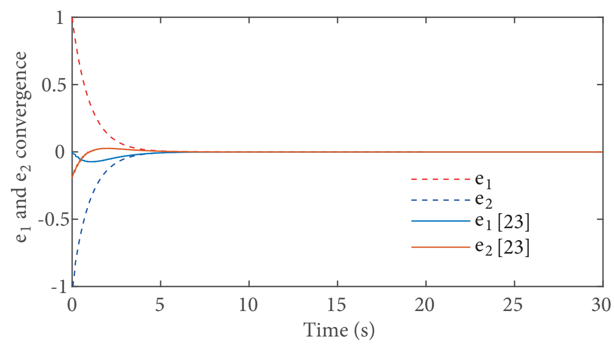

Figure 8. The error convergence via adaptive ISMC and backstepping strategy [23].

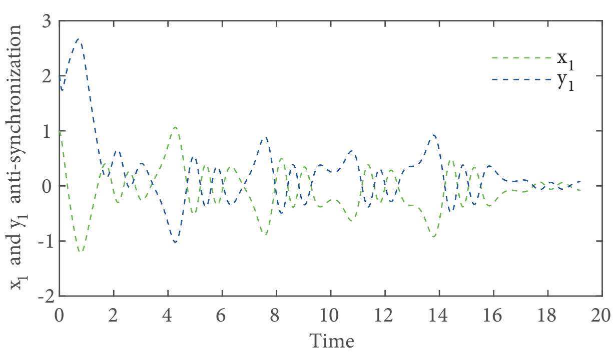

Figure 9. The antisynchronization of the position variables under the action of adaptive ISMC.

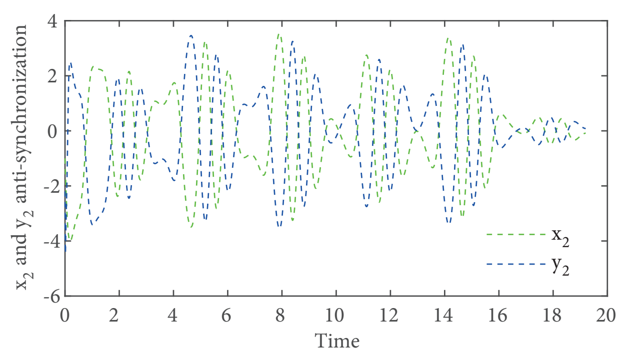

Figure 10. The antisynchronization of the velocities under the action of adaptive ISMC.

References

[1] Ott E, Grebogi C, Yorke JA. Controlling chaos. Phys Rev Lett 1990; 64: 1196-1199.

[2] Pecora LM, Carroll TL. Synchronization in chaotic systems. Phys Rev Lett 1990; 64: 821-824.

[3] Kapitaniak T. Controlling Chaos-Theoretical Practical Methods in Non-linear Dynamics. London, UK: Academic Press, 1996.

[4] Chen G, Dong X. From Chaos to Order: Methodologies, Perspectives and Applications. Singapore: World Scientific, 1998.

[5] Pikovsky AS, Rosenblum MG, Kurths J. Synchronization - A Unified Approach to Nonlinear Science. Cambridge, UK: Cambridge University Press, 2001.

[6] Yu X, Song Y. Chaos synchronization via controlling partial state of chaotic 16 systems. Int J Bifurcat Chaos 2001; 11: 1737-1741.

[7] Wang C, Ge SS. Adaptive synchronization of uncertain chaotic systems via backstepping design. Chaos Soliton Fractal 2001; 212: 1199-1206.

[8] Laoye JA, Vincent UE, Kareem SO. Chaos control of 4-D chaotic system using recursive backstepping nonlinear controller. Chaos Soliton Fractal 2009, 41: 2371-2376.

[9] Yassen MT. Chaos synchronization between two different chaotic systems using active control. Chaos Soliton Fractal 2005; 23: 131-140.

[10] Ling L, Zhi AG, Chao Z. Synchronization between two different chaotic systems with nonlinear feedback control. Chin Phys Soc 2007; 16: 1603-1607.

[11] Yang W, Xia X, Dong Y, Zheng S. Finite time synchronization between two different chaotic systems with uncertain parameters. Comp Info Science 2010; 3: 174-179.

[12] Sahab AR, Taleb ZM. Adaptive generalization backstepping method to synchronize T-system. In: WSEAS 2011 Applied, Numerical and Computational Mathematics Conference; 15–17 September 2011; Barcelona, Spain. pp. 102-109.

[13] Yu F, Wang C, Hu Y, Yin J. Antisynchronization of a novel hyperchaotic system with parameter mismatch and external disturbances. Pramana J Phys 2012; 12: 81-93.

[14] Fang L, Li T, Wang X, Gao X. Adaptive synchronization of uncertain chaotic systems via neural network based dynamic surface control design. In: Guo C, Hou ZG, Zeng Z, editors. Advances in Neural Networks. Berlin, Germany: Springer, 2013. pp. 104-111.

[15] Sundarapandian V, Sivaperumal S. Global chaos synchronization of the hyperchaotic qi systems by sliding mode control. Int J Comput Sci Eng 2011; 3: 2430–2437.

[16] Zhang BJ, Li HX. A new four-dimensional autonomous hyper chaotic system and the synchronization of different chaotic systems by using fast terminal sliding mode control. Math Probl Eng 2013; 2013: 179428.

[17] Lin TC, Chen MC, Roopaei M. Synchronization of uncertain chaotic systems based on adaptive type-2 fuzzy sliding mode control. Eng Appl Artif Intell 2011; 24: 39–49.

[18] Fang L, Li T, Li Z, Li R. Adaptive terminal sliding mode control for anti-synchronization of uncertain chaotic systems. Nonlinear Dyn 2013; 74: 991–1002.

[19] Utkin VI, Guldner J, Shi J. Sliding Mode Control in Electromechanical Systems. London, UK: Taylor & Francis, 1999.

[20] Levant A. Higher-order sliding modes, differentiation and output-feedback control. Int J Cont 2003; 76: 924–941.

[21] Chang JL. Dynamic output integral sliding-mode control with disturbance attenuation. IEEE T Aut Cont 2009; 54: 2653–2658.

[22] Khan Q, Akmeliawati R. Neuro-adaptive dynamic integral sliding mode control design with output differentiation observer for uncertain higher order MIMO nonlinear systems. Neurocomputing 2017; 226: 126-134.

[23] Idowu BA, Vincent UE, Njah AN, Control and synchronization of chaos in nonlinear gyros via backstepping design. Int J Nonlinear Sci 2008; 5: 11-19.

[24] Chen HK, Chaos and chaos synchronization of a symmetric gyro with linear-plus-cubic damping. J Sound Vib 2002; 255: 719-740.